Available online at www.sciencedirect.com
ScienceDirect
Thin Solid Films 515 (2007) 6557–6561
www.elsevier.com/locate/tsf

Effects of porosity on ferroelectric properties of $Pb(Zr_{0.2}Ti_{0.8})O_3$ films

V. Stancu [b,*], M. Lisca [b], I. Boerasu [c], L. Pintilie [a], M. Kosec [c]

[a] *Max Planck Institute of Microstructure Physics, Weinberg 2, Halle, 06129 Germany*
[b] *National Institute of Materials Physics Bucharest-Magurele, P. O. Box MG-7, 77125, Romania*
[c] *Josef Stefan Institute, Jamova 39, 1000 Ljubljana, Slovenia*

Available online 25 January 2007

Abstract

The sol–gel deposition method has been successfully applied to obtain $Pb(Zr_{0.2}Ti_{0.8})O_3$ thin films on platinized silicon wafers. Addition of different amounts (7–15 wt.%) of organic macromolecular polyvinylpyrrolidone in the precursor solution prior to spin coating proves to be an excellent method for obtaining porous films. The crystal structure of as deposited films was analyzed by X-ray diffraction. The porous films show perovskite phase after annealing at 650 °C. The surface morphology has been studied by Atomic Force Microscopy and Scanning Electron Microscopy. The surface profile indicates a roughness of the film of 5 nm and no microcracks on the surface. The ferroelectric behavior was proved for each film, by hysteresis loops and by the "butterfly" shape of the capacitance–voltage characteristics. The remnant polarization and the coercive field decrease while the amount of added PVP increases.

Keywords: PZT; Porous thin films; PVP; Ferroelectric

1. Introduction

Polar dielectrics, particularly ferroelectrics, possess many interesting properties that are applied widely in electronics, such as non-volatile memories, field effect devices, piezoelectric transducers and heat sensors, capacitors etc. [1]. Thin films of this class of materials, mainly ferroelectric oxides such as Pb(Zr, Ti)O_3 (Ba,Sr)TiO_3 and $SrBi_2Ta_2O_9$, have been studied intensively over the last 15 years [2–4]. Pyroelectric thin films have many applications in temperature sensing systems for fire and intruder detection, air condition control and thermal imaging [5].

Several methods have been developed to prepare ferroelectric thin films, such as RF sputtering, metal–organic chemical deposition, electron beam evaporation, pulsed laser deposition, sol–gel method [6,7]. Among these methods, the sol–gel process is widely used due to its good reproducibility, low cost and uniform as-deposited film thickness. Most of the sol–gel work reported in the literature employs a process first reported in 1985 [7]. The sol–gel method involves the preparation of sol precursor which is applied to a support substrate by the spin-coating technique. The deposited layers are thermally annealed in order to obtain the ferroelectric thin film.

Chemical and physical phenomena can influence the ferroelectric properties of thin films. One way to improve the pyroelectric devices performances is the "artificial" change of physical properties of Pb(Zr,Ti)O_3 (PZT) materials. The quality of a pyroelectric material is evaluated based on its figures of merit, which are: $F_v = p/\varepsilon_r$ for voltage mode operation, in which case it is necessary to maximize the pyroelectric coefficient p and lower the permittivity; $F_d = p/(\varepsilon_r \tan\delta)^{1/2}$ for the current mode operation, in which the dielectric loss ($\tan\delta$) becomes important. A method to increase the figures of merit is to prepare porous films, with lower ε_r. The porous ferroelectric studies showed that the porosity is influenced by the annealing rate [8] or the nature of the doping into the solid solution of $PbTiO_3$–$PbZrO_3$ [9]. Suyal and Setter [10] reported strong dependence between dielectric constant and the porosity of the films.

This paper presents the sol–gel method used to prepare PZT porous thin films on platinized silicon substrate by adding polymer polyvinylpirrolidone (PVP) in the precursor solution. The sol–gel process, dielectric and ferroelectric characterization of the porous films will be discussed in the following sections. It will be shown that ferroelectric properties of the porous films

* Corresponding author. Tel.: +40 21 4930195; fax: +40 21 4930267.
E-mail address: stancu@infim.ro (V. Stancu).

0040-6090/$ - see front matter © 2006 Elsevier B.V. All rights reserved.
doi:10.1016/j.tsf.2006.11.165

are changed with respect to the properties of the dense films deposited on standard Pt-coated silicon.

2. Experimental procedure

PZT thin films were prepared from alkoxide precursor by sol–gel method. Fig. 1 illustrates the synthesis of PZT. The process starts from alcoxide precursors: lead acetate Pb $(CH_3COO)_2{\cdot}3H_2O$ (Reactivul Bucuresti), zirconium *n*-propoxide $Zr[O(CH_2)_2CH_3]_4$ (Alfa) and titanium isopropoxide Ti $[OCH(CH_3)_2]_4$ (Alfa) dissolved in solvent 2-methoxyethanol (Aldrich). A solution with a Zr/Ti ratio of 20/80 and containing 5% excess of lead precursor was prepared. The PVP polymer (Merck), with M.W.=25.000, was dissolved in the PZT solution under stirring condition in 7–15 wt.% in order to modify the porosity.

The solution of starting reagents was prepared in dry atmosphere (N_2). In order to eliminate the water, the lead, zirconium and titanium precursors were separately distilled. Definite volumes of lead, zirconium and titanium precursor solutions were mixed in 2-methoxyethanol medium. In this solvent the lead acetate reacts with the transition metal alkoxides by elimination of esters. The resulting solution was two times distilled in order to complete the reaction and totally remove the reaction by-products. The PZT final solution had the (1 M) concentration. For film deposition, the PZT sol was diluted to 0.5 M with solvent. PVP $(C_6H_9NO)_n$ was added to precursor solution (0.5 M) in 7, 10, 12, 15 wt.% to get different porosities in the films (samples P1, P2, P3, P4). Sample P5 is the dense PZT film prepared in the same condition as porous samples, but without PVP addition to precursor solution.

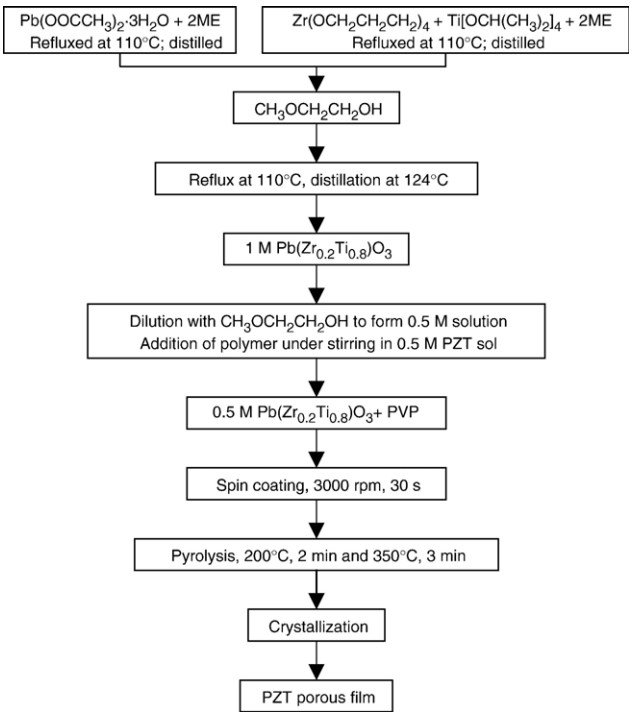

Fig. 1. Flow diagram for the sol–gel processing of PZT porous films.

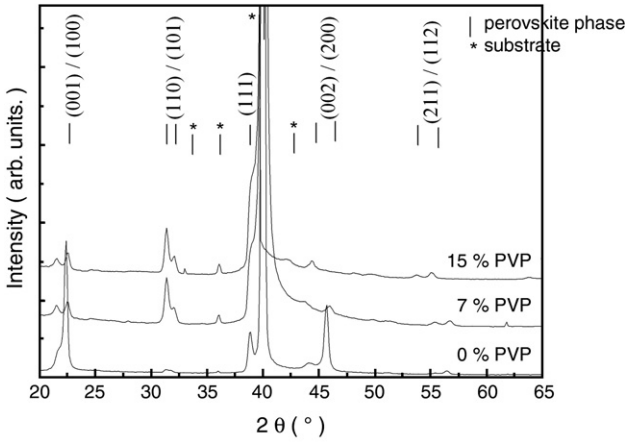

Fig. 2. X-ray diffraction patterns of PZT films.

PZT thin film was deposited on platinized silicon substrate ($Pt/TiO_2/SiO_2/Si$) by spin coating at 3000 rpm for 30 s. The film was pyrolized at two different temperatures: 200 °C/2 min and 350 °C/3 min, and crystallized by Conventional Thermal Annealing (CTA) at 650 °C/30 min using a heating rate of 5 °C/min.

The crystalline phases in the PZT thin films were identified by X-ray diffraction (XRD) in 2θ geometry, using Cu Kα radiation. The microstructure of the films was investigated by Scanning Electron Microscopy (SEM) and Atomic Force Microscopy (AFM). Gold electrodes were deposited by thermal evaporation through a shadow mask onto the surface of PZT thin films, with an area of 1.5 mm^2. The structures obtained in this manner are asymmetric: the bottom electrode is platinum and the top electrode is gold.

The dielectric constants of the samples were estimated from the capacitance–voltage (C–V) characteristics measured at 1 kHz with an Agillent LCR meter. Hysteresis measurements were made using a RT66A analyzer at 100 Hz, while the current–voltage characteristics were recorded using a computer controlled Keithley 6517 A electrometer. All measurements were performed at room temperature.

3. Results and discussions

The XRD results for the dense PZT thin film and for PZT films with two different PVP polymer weight percentages added to precursor solution are shown in Fig. 2. The PZT dense film shows predominant tetragonal perovskite phase. In the porous materials it is noticed the substantial presence of (110) orientation. The perovskite structure of PZT films is evidenced by the splitting of the (001)/(100), (002)/(200) peaks. The X-ray analysis of the porous films, after heat-treatment at 650 °C, proved the absence of PVP indicating that the polymer was well decomposed.

The surface microstructure of the PZT porous films deposited on the Pt/Si substrates is shown in Fig. 3(a). The SEM analysis showed a crack-free surface and porous microstructure. The thickness of the films were estimated from Scanning Electron Microscopy, cross-section view, made on freshly fractured

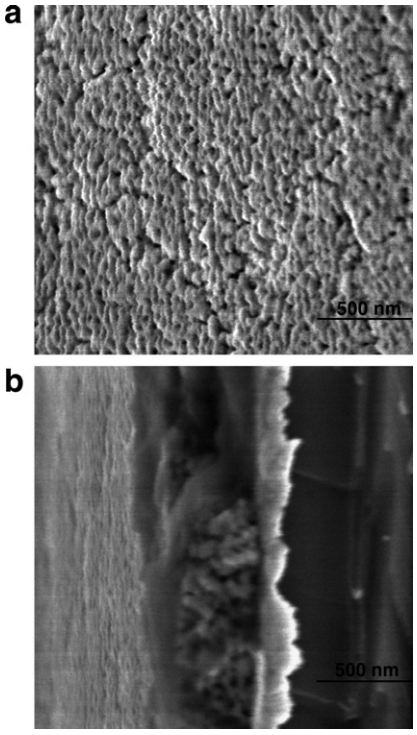

Fig. 3. SEM images of PZT porous film deposited on Pt/Si substrate (sample P2): (a) plan view (b) cross-section view.

surfaces and the values are given in Table 1 together with other characteristic values of the films. An example of cross-section view is presented in Fig. 3(b) and shows that there are no pores going from the top to the bottom of the film, the pores are small and relatively uniform distributed into the film. These features are valid for all porous materials presented in this paper, only the size of pores is different for each sample. The pores size increases by increasing the amount of polymer added to precursor solution, and this fact has an effect on the final film thickness. Kozuka and Kajimura [11] reported the effect of polyvinylpyrrolidone on the thickness of the sol–gel deposited films. It has been demonstrated that the PVP can suppress the condensation reaction during the heat treatment and consequently improve the thickness of the films. In our opinion, there are two concurring phenomena which affect the final thickness of the film. First is the fact that the addition of the PVP makes the starting solution more viscous. That will lead to an increased thickness after crystallization. The second phenomena is the formation of the pores by the PVP decomposition. The pores size increases with increasing the PVP content. The larger holes between the PZT crystallites can lead to a shrinkage of the film during crystallization annealing. Thus, the final film thickness increases at small addition of PVP (see samples P1 and P2) because of increased viscosity, then decreases at larger addition of PVP (see samples P3 and P4) because of larger pores causing shrinkage during crystallization. The PVP content is thus an important parameter for the final thickness of the films. When PVP is added into the precursor it can hybridize with metalloxane polymer through strong hydrogen bonding between C═O group of PVP and the OH group of the metalloxane

Table 1
Characteristics of porous and dense PZT films.

	Thickness (nm)	P_{rm} (μC/cm)	E_{cm} (kV/cm)	ε_{film}	Porosity (%)
P1 (7 wt.% PVP)	380	9.2	250	42.37	40
P2 (10 wt.% PVP)	500	3.55	148.8	83.99	30
P3 (12 wt.% PVP)	370	5.6	173	102.84	25
P4 (15 wt.% PVP)	300	7.4	220	118.19	20
P5 (without PVP)	250	28.65	163	246.32	0

polymer. The C═O group can suppress the condensation reaction and promote the structural relaxation. PVP is a polymer material with a molecular weight higher than any other organic material used in the precursors. Therefore the pores occur by the PVP pyrolysis [12]. This statement is supported by the results of the Thermo-gravimetric/Differential Thermal Analysis (TG/DTA) analysis performed on the PZT–PVP precursor solution, shown in the Fig. 4. Three weight losses can be observed up to 550 °C, due to the decomposition of the organic products, including polymeric PVP, and elimination of water, carbon dioxide and nitrogen dioxide. No weight loss is observed above 550 °C, suggesting that PVP decomposition is completed at this temperature, when the PZT crystallization starts [11].

The AFM analysis confirmed the facts observed by Scanning Electron Microscopy on the film surfaces. An example of surface view, made by AFM, is presented in Fig. 5. All the PZT films deposited on Pt/Si have a smooth surface with an average roughness of 4–5 nm.

In order to probe the films ferroelectric behaviour, a set of electric measurements were performed, like hysteresis loops, capacitance–voltage (C–V) and current–voltage (I–V) characteristics.

The hysteresis loops were measured at 100 Hz for each sample. These are presented in Fig. 6. The porous films present hysteresis loops with remnant polarization values lower than the value for the PZT dense film. All the films show some asymmetry, which can be related to the electrode asymmetry (different work functions for the bottom platinum and the top gold electrodes) [13]. However, the degree of asymmetry might

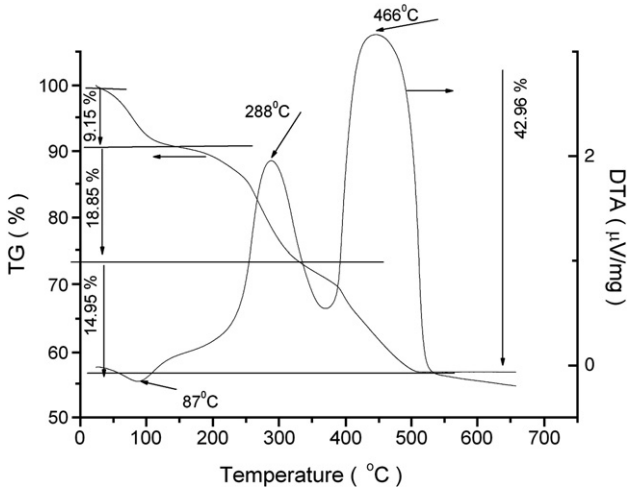

Fig. 4. TGA/DTA analysis of PZT+7 wt.% PVP.

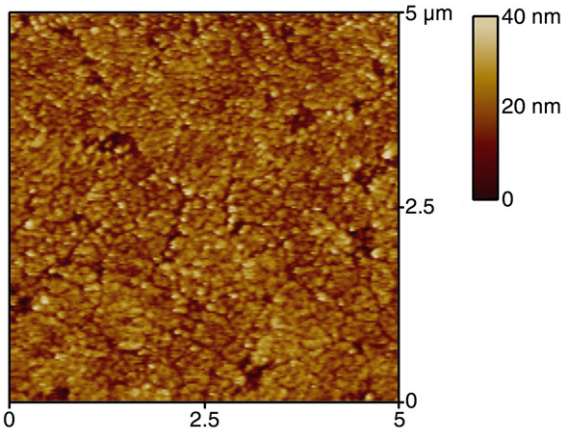

Fig. 5. AFM picture of sample P1. Investigated area is $5 \times 5\ \mu m^2$.

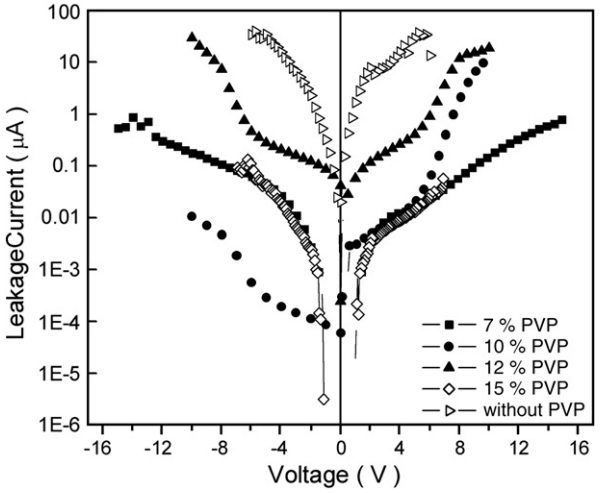

Fig. 7. Current–Voltage characteristics for investigated ferroelectric thin films.

be influenced by the porosity, as the presence of the pores beneath the electrodes can change the interface properties. Polarization reversal in case of porous PZT films is gradual and is a consequence of having different orientations of crystallites, as can be seen in the X-ray diffraction patterns. The dense PZT film is orientated in one direction, having then a faster polarization reversal and a shape of the hysteresis loop closer to rectangle. The values of the remnant polarization (P_r) and coercive field (E_c) were extracted for each sample from the hysteresis loops, and are also presented in Table 1. The loops are not well compensated and saturated because of the high leakage currents, which adds parasitic contribution to the charge integrated by the RT66 analyzer. The parasitic contribution of the leakage current increases non-linearly with the applied voltage, as can be seen from the current–voltage characteristics presented in Fig. 7. This fact makes difficult to evidence the polarization saturation in the hysteresis loops, even the applied voltage was raised to 20 V.

The high leakage currents, with disperse values, make difficult to extract any useful information about the influence of added polymer on the *I–V* characteristics of porous thin films.

As mentioned above, the pores presence beneath the electrodes can influence the electrode/PZT interface properties, with direct impact on the leakage current.

The capacitance–voltage characteristics shown in Fig. 8 have the "butterfly shape" characteristic for ferroelectric materials. The capacitance peaks are directly related to the switching of the ferroelectric polarization [14]. These are broad enough in each case, suggesting a gradual reversal process which is in accordance with the hysteresis loops shown in Fig. 6. The capacitance values of porous films are lower than the PZT dense film and they strongly decrease by decreasing the amount of PVP added to the precursor solution. The dielectric constant for each sample was calculated from the measured capacitance at 0 bias, by using the plan-parallel capacitor model. The obtained values are given in Table 1. The decrease of the dielectric constant in porous PZT 20/80 films suggests their potential for pyroelectric applications. Assuming that the pyroelectric coefficient is about the same in porous and dense films, we can expect a larger figure of merit in the case of the porous films because of the lower dielectric constant.

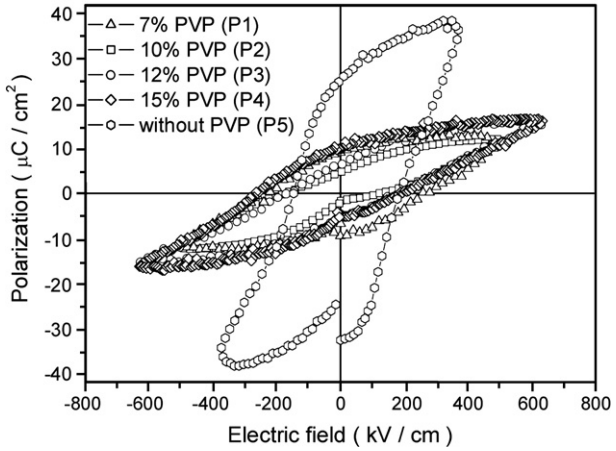

Fig. 6. Hysteresis loops for porous PZT 20/80 thin films made at room temperature and frequency of 100 Hz.

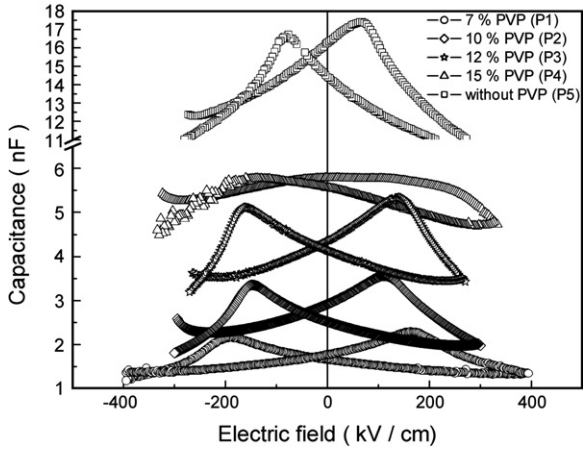

Fig. 8. *C–V* characteristics of the porous and dense PZT thin films deposited on Pt/Si, at 1 kHz.

The *spherical bubbles* model was applied [15] to extract the PZT films porosities.

$$\varepsilon_{\text{efectiv}} = \left(1 - \frac{3p}{2+p}\right)\varepsilon_{\text{b}} + \frac{3p}{2+p}\frac{3\varepsilon_p\varepsilon_{\text{b}}}{(2+p)\varepsilon_{\text{p}} + (1-p)\varepsilon_{\text{b}}}. \quad (1)$$

$\varepsilon_{\text{efectiv}}$ is the dielectric permittivity of composite, ε_{b} is the dielectric permittivity of PZT grain bulk, $\varepsilon_{\text{p}}=1$ is the dielectric permittivity of pores, assumed to be filled with air, and p is the generalized film porosity, i.e. macro-porosity, nano-porosity or cracks. Several procedures of porosity calculation have been reported by literature [13,16]. We have used an analytic approach to estimate the amount of porosity in deposited films. Considering that the dielectric permittivity of PZT grain bulk is equal with dielectric permittivity of the PZT dense film, $\varepsilon_{\text{PZTfilm}}=246$, then the p coefficient can be estimated from Eq. (1). The porosity values are given in Table 1. It can be observed that the porosity decreases with increasing the amount of added PVP, which is an unexpected result. Normally, it should be expected that the porosity increases with increasing the PVP content in the precursor solution. This apparent contradiction can be explained on the basis of SEM investigations, showing that the increase of the PVP content leads to larger pores, in lower concentration. Large pores might favor the densification of the films during the annealing process, leading to a lower thickness, lower porosity and higher capacitance than for the sample with the lowest content of PVP (7 wt.%). Thus, the results on porosity estimation correlate well with the capacitance measurements, showing the lowest capacitance value for the film with the highest porosity (the porosity was expressed as volume percentage). This is the film with the lowest amount of PVP.

4. Conclusion

The use of PVP as a volatile phase proves to be an excellent method for introducing a porous microstructure in PZT films. These porous films still present ferroelectric properties and have different material characteristics. The porosity increases with decreasing the PVP content in the precursor solution, leading to a lower dielectric constant of the porous PZT films. These are good candidates for pyroelectric applications.

Acknowledgement

This work was funded through CERES 4-252 “FENAPOFS” Project of the Romanian Ministry of Education and Research.

References

[1] J.F. Scott, in: Advanced Microelectronics Series (Ed), Ferroelectric Memories, Springer–Verlag Berlin Heidelberg, 2000.
[2] S. Bhattacharyya, A. Laha, S.B. Krupanidhi, J. Appl. Phys. 91 (7) (2002) 4643.
[3] F.M. Pontes, D.S.L. Pontes, E.R. Leite, E. Longo, A.J. Chiquito, P.S. Pizani, J.A. Varela, J. Appl. Phys. 94 (2003) 7256.
[4] H. Morioka, S. Yokoyama, T. Oikawa, H. Funakubo, K. Saito, Appl. Phys. Lett. 85 (16) (2004) 3516.
[5] R.W. Whatmore, Rep. Prog. Phys. 49 (1986) 1335.
[6] W. Braun, B.S. Kwak, A. Erbil, J.D. Budai, B.J. Wilkens, Appl. Phys. Lett. 63 (1993) 467.
[7] K.D. Budd, S.K. Dey, D.A. Payne, Br. Ceram. Proc. 36 (1985) 107.
[8] P. Muralt, Rep. Prog. Phys. 64 (2001) 1339.
[9] A. Seifert, J. Sol–Gel Sci. Technol. 16 (1999) 13.
[10] G. Suyal, N. Setter, J. Eur. Ceram. Soc. 24 (2004) 247.
[11] H. Kozuka, M. Kajimura, J. Am. Ceram. Soc. 83 (2000) 1056.
[12] Z. Wang, J. Liu, T. Ren, L. liu, Sens. Actuators, A 117 (2005) 293.
[13] I. Rychetsky, J. Petzelt, T. Ostapchuk, J. Appl. Phys. 81 (2002) 4224.
[14] L. Pintilie, M. Lisca, M. Alexe, Proceedings of the 27th International Semiconductor Conference, Sinaia, Romania, Oct 4–6 2004, p. 415.
[15] L. Pintilie, M. Lisca, M. Alexe, Appl. Phys. Lett. 86 (2005) 192902.
[16] A. Seifert, P. Muralt, N. Setter, J. Appl. Phys. 72 (1998) 2409.